Giant Stokes fields on semicontinuous metal films

Patrice Gadenne

Laboratoire de Magnetisme et d'Optique de Versailles, Universite de Versailles Saint-Quentin, 78035 Versailles cedex, France

F. Brouers

Etude Physique des materiaux et Genie Chimique University de Liege B5, 4000 Liege, Belgium

Vladimir M. Shalaev

Department of Physics, New Mexico University, Las Cruces, New Mexico 88003

Andrey K. Sarychev

Center for Applied Problems of Electrodynamics, Russian Academy of Sciences, Moscow 127412, Russia

Received May 6, 1997; revised manuscript received August 18, 1997

The local electric fields on a semicontinuous metal film are shown to experience giant fluctuations in the visible and infrared spectral ranges when the dissipation in metallic grains is small. The field fluctuations result in strongly enhanced Raman scattering. The scattered local fields at the Stokes frequency are concentrated in sharp well-separated peaks and are enhanced up to giant values, $\sim 10^{14}$, that exceed by many orders of magnitude the average enhancement, $\sim 10^{6}$. This opens a fascinating possibility for Raman scattering spectroscopy of single molecules on a semicontinuous metal film. A developed scaling theory for surface-enhanced Raman scattering from a semicontinuous film successfully explains the experimental observations. © 1998 Optical Society of America [S0740-3224(98)01301-0]

OCIS codes: 290.5860, 300.0300, 350.6670.

The optical properties of metal-dielectric thin films are of great interest, in large part because of their high potential for various applications. Two-dimensional semicontinuous metal films are usually produced by thermal evaporation or sputtering of metal onto an insulating (dielectric) substrate. In the growing process, first, small metallic grains are formed on the substrate. As the film grows, the metal concentration increases and coalescences occur; thus irregularly shaped clusters are formed on the substrate, eventually resulting in two-dimensional fractal structures. At the percolation threshold a continuous conducting path of metal appears between the ends of the sample. At higher surface coverage the film is mostly metallic, with voids of irregular shapes. As further coverage increases, the film becomes uniform.

Metal-dielectric films manifest anomalous phenomena that are absent for bulk metal and dielectric components. For example, the anomalous absorption in the near-infrared spectral range leads to unusual behavior of the transmittance and reflectance (see Refs. 1–4 and references therein). Despite a large amount of theoretical work on electromagnetic properties of random films (see, for example, Refs. 2–4), little attention has been paid so far to the field fluctuations and effects resulting from these fluctuations.

In this paper we show that the local electromagnetic fields experience huge fluctuations on a semicontinuous metal film resulting in giant surface-enhanced Raman scattering (SERS), with the SERS centers localized in very small, nanometer-sized areas of the film. Single-molecule SERS from colloidal particles and their aggregates was recently reported.[5,6] We show here that a semicontinuous metal film can be also used for spectroscopy of single molecules based on SERS.

SERS from various nanostructured materials (rough films, colloidal aggregates, etc.) is one of most intriguing optical effects discovered in the past two decades.[7] Recent studies[8,9] indicate that SERS is especially large in strongly disordered media, such as fractal small-particle composites and self-affine thin films, where the local-field fluctuations are especially large because of spatial localization of optical modes in different random parts of the object.[10,11] As known, near the percolation threshold of a semicontinuous film, field fluctuations are also very large; therefore SERS is anticipated to experience giant enhancement in this case.

In most studies the average (integrated) SERS was considered. In this paper we show that for SERS from a semicontinuous film, the distributions of local fields at the Stokes frequency consist of sharp nanometer-sized peaks that are localized in spatially separated areas of the film. The enhancement in the peaks exceeds the average enhancement by many orders of magnitude; this is because the local peaks of SERS are separated by distances much larger than the peak sizes. The near-field effects in SERS from metal semicontinuous films discussed in this paper can be obtained, for example, by means of near-field scanning optical microscopy providing subwavelength

0740-3224/98/010068-05$10.00

resolution[12]; in particular, based on the reported results, we anticipate that previous studies on near-field scanning optical spectroscopy of a single molecule[13] can be developed to include SERS from single molecules.

To simplify theoretical considerations, we assume below that the skin depth for the metal grains is much larger than the grain size, so that the quasistatic approximation holds. For most of metals the real part, ε_m', of the complex dielectric constant, $\varepsilon_m = \varepsilon_m' + i\varepsilon_m''$, is negative (and large in modulus) in the visible and infrared spectral ranges, whereas the losses are small, $\kappa = \varepsilon_m''/|\varepsilon_m'| \ll 1$. At the percolation the effective dielectric constant, $\varepsilon_e = \sqrt{\varepsilon_m \varepsilon_d}$, is purely imaginary if we neglect the metal losses and possible small losses in the dielectric substrate.[14] Therefore a film consisting of loss-free metal and dielectric grains is absorptive. The effective absorption in a loss-free film means that the electromagnetic energy is stored in the system and thus the local fields could increase unlimitedly; in reality, the local fields in a metal film are, of course, finite because of the small losses. From this simple consideration one anticipates very strong field fluctuations in random metal film with small losses.

We calculate the field distribution on a semicontinuous film using a very effective numerical method.[15] In this method one applies the real-space renormalization group (RSRG) approach suggested by Reynolds *et al.* and Sarychev.[16] The method can be also adopted to finding the field distributions.[15] It is based on generating a square lattice of L–R (metal) and C (dielectric) bonds using a random-number generator. After using the RSRG transformation,[15] we apply an external field to the system and solve the Kirchhoff equations to determine the fields and the currents in all the bonds of the transformed lattice. Owing to the hierarchical structure of the transformed lattice, these equations can be solved exactly. Then we use the one-to-one correspondence between the elementary bonds of the transformed lattice and the bonds of the initial square lattice to find the field distributions in the initial lattice as well as its effective conductivity. In our numerical calculations the system size was 1024×1024.

The metal dielectric constant is chosen to have the Drude form, $\varepsilon_m(\omega) = \varepsilon_b - (\omega_p/\omega)^2/(1 + i\omega_\tau/\omega)$, where ε_b is a contribution to the ε owing to inter-band transitions, ω_p is the plasma frequency, and $\omega_\tau = 1/\tau \ll \omega_p$ is the relaxation rate. The consideration below is limited to the frequency range $\omega_\tau \ll \omega \leqslant \omega_p$.

In accordance with the above arguments, our numerical calculations demonstrate the large fluctuations for the intensity, $I(x, y) = |E(x, y)|^2 \gg |E_0|^2$ ($E_0 = 1$ is the macroscopic applied field), of the local electric field, $E(x, y)$, when the (fundamental) frequency of the applied field, ω, is smaller than the renormalized plasma frequency, $\omega_p^* = \omega_p/\sqrt{\varepsilon_b}$. For example, for silver semicontinuous films ($\varepsilon_b = 5.1$, $\omega_p = 9.1$ eV, $\omega_\tau = 0.021$ eV) on a glass substrate ($\varepsilon_d = 2.2$), the field intensity $I(x, y)$ is up to $\sim 10^5$ in the peaks and $\sim 10^2$, on average, at the wavelength $\lambda = 1.5$ μm. According to results of our numerical simulations (not shown), the local intensity, $I(x, y)$, at the fundamental frequency is highly inhomogeneous in space and concentrated in sharp, well-separated peaks. The local fields are enhanced because of the excitation of the film eigenmodes.

The strong-field fluctuations at the fundamental frequency result in giant enhancement of Raman scattering. Raman scattering from a semicontinuous film can be thought of as a two-stage process. First, strong-field fluctuations at the fundamental frequency, ω, of the applied field induce the Stokes dipoles (currents) in Raman-active molecules placed on the surface of the film. Then the Raman-active molecules serve as secondary sources exciting the resonant currents in metal grains at the Stokes-shifted frequency, ω_s. Because of this double enhancement associated with the resonant currents at the fundamental and Stokes frequency, the local SERS is proportional to the fourth power of the local fields,[7,8,15] $|E(x, y)|^4$, provided the Stokes shift of frequency is small, $|\omega - \omega_s| \ll \omega$. Further, since the Stokes fields from different molecules include random phases, the Raman currents that they excite in the film are also incoherent and can be considered as independent local sources of SERS. In accordance with these arguments the enhancement factor for Raman scattering from a semicontinuous film, A, can be written as

$$A = |T(p)|^2 \int I_R(x, y)\,dx\,dy/(|E_0|^4 \varepsilon_d{}^2), \qquad (1)$$

where $I_R(x, y) = |\varepsilon(x, y)|^2 |E(x, y)|^4$ is the local Raman current at the Stokes frequency and T is the film transmittance. The enhancement A in Eq. (1) is defined as the ratio of Raman signals from a film (covered by Raman-active molecules) with and without metal grains on it. The prefactor $|T|^2$ in Eq. (1) takes into account that the macroscopic field in the film, E_0, differs from the field, E_{inc}, of the incident wave: $E_0 = TE_{\text{inc}}$.

Using the described above numerical method based on the RSRG approach, we calculated distributions of the local Raman currents, $I_R(x, y)$, in a silver semicontinuous film at $p = p_c$; the results are shown in Fig. 1 for different wavelengths. The quantity $I_R(x, y)$ characterizes the local SERS enhancement [see Eq. (1), where $E_0, T, \varepsilon_d \approx 1$]. As seen in the figure, the local enhancements have the forms of sharp peaks sparsely distributed on the film, with the magnitudes increasing toward the long-wavelength part of the spectrum. The enhancement in peaks achieve $\sim 10^9$ for $\lambda = 1.5$ μm, $\sim 10^{11}$ for $\lambda = 10$ μm, and $\sim 10^{14}$ for $\lambda = 20$ μm. The average enhancement, A, is much less, of the order of 10^6, for all the wavelengths (see below).

As seen in the figure, the peak positions strongly depend on the frequency. This nontrivial pattern for the local SERS distribution can be probed by means of near-field scanning optical spectroscopy. If the density of Raman-active molecules is small enough, then each peak in Fig. 1 is due to Raman scattering from a single molecule. Thus the presented picture of the SERS distribution opens a unique opportunity to perform Raman spectroscopy of a single molecule on a semicontinuous metal film.

The obtained distribution for the local SERS results from strong fluctuations of the local fields (and currents) near the percolation threshold. Since the enhancement is proportional to the local field raised to the fourth

power, the largest contribution to the SERS signal comes from small areas where the fluctuating fields are especially high. These areas of large local fields are associated with the film eigenmodes that resonate at a given laser wavelength λ. When λ is changed, new eigenmodes of a film are excited, resulting again in the high local fields in the areas where the modes are located.

Note that all results are shown in the natural linear scales; therefore what we see in the figures is a top part of the SERS distribution, i.e., only the largest Stokes fields. The fields at other points forming a background, although smaller, are not, of course, zero (they cannot be seen simply because they are much smaller than the maximum fields). However, since the SERS $\propto |E(x, y)|^4$, only the largest fields play an important role, and the smaller background fields (not seen in the figures) do not contribute much to the signal.

For high frequencies, $\omega \approx \omega_p^*$ (for silver, $\lambda_p = 0.364$ nm), one expects that the local fields experience giant fluctuations; this is because at these frequencies, the real part of the metal dielectric constant, ε_m', is negative and its absolute values are of the order of ε_d. Therefore at these frequencies the plasmon resonance is effective for each of the metal grains that almost do not interact, provided p is well below p_c. At $p \approx p_c$ the particles' interactions become important; these interactions shift the resonance and thus suppress the induced currents and the corresponding local fields. In accordance

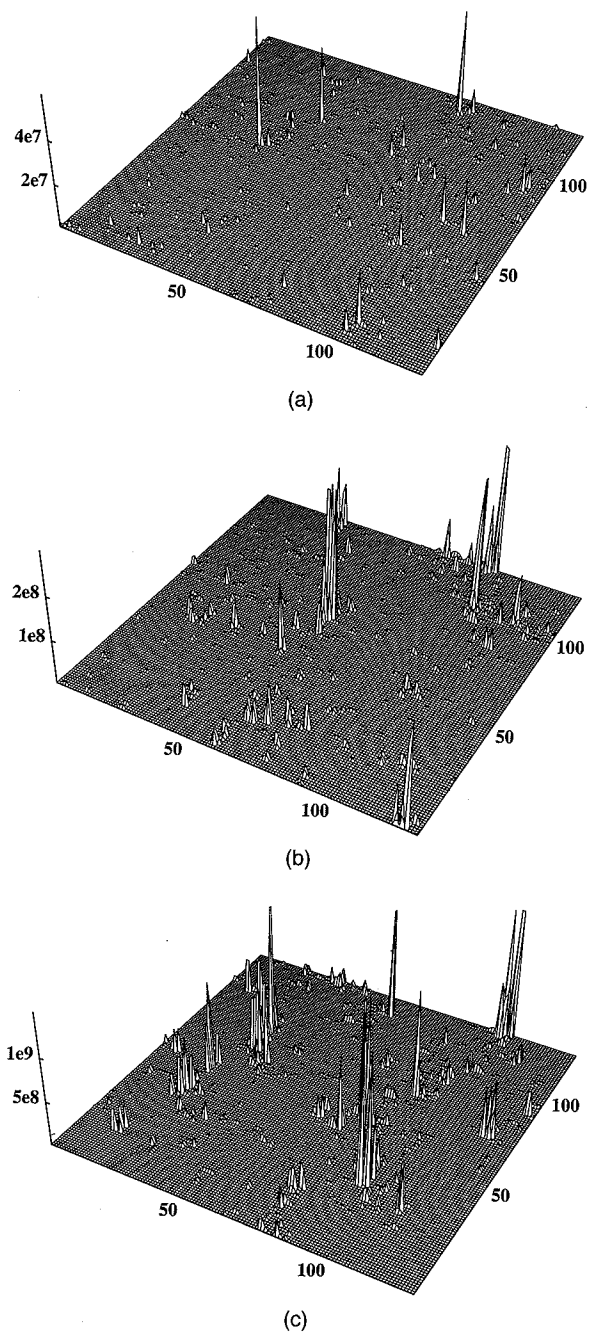

Fig. 1. Distributions of the local enhancements of Raman scattering on a silver semicontinuous film at the percolation threshold for different wavelengths: (a) λ = 0.36 μm, (b) λ = 0.5 μm, (c) λ = 1.5 μm, (d) λ = 10 μm, and (e) λ = 20 μm.

with this, SERS also decreases at $p \approx p_c$. However, for higher metal concentrations, $p \to 1$, the plasmon resonance associated with sparse dielectric voids (that almost do not interact at p close to 1) becomes effective, so that the local fields and corresponding SERS increase again at the larger p. Finally, at $p = 1$ the field fluctuations are absent and SERS is small. This double-maximum behavior in the SERS dependence on p is observed in our experiment reported in this paper and is in agreement with our numerical calculations based on formula (1). The results of our numerical simulations (averaged over ten realizations) and experimental data are shown in Fig. 2.

In our experiments, silver thin films were deposited on glass substrates at room temperature under ultrahigh vacuum (10^{-9} Torr). In order to determine a closeness to the percolation threshold, the resistivity and the deposited mass thickness were measured all along the film deposition. Optical reflection and transmission of the samples were also determined out of the vacuum chamber and compared with the well-known optical properties of percolating samples.[17] Transmission electron microscopy was performed afterward by stripping a small part of the deposit out of the substrate. In order to adsorb the Raman-active molecules of zinc tetraphenypropilene on the surface of the silver grains, we used the procedure described by Corton and Schlegel.[18] The Raman signal was measured with a triple monochromator of 12-cm^{-1} bandwidth. As a light source we used an Ar^+ laser with wavelength $\lambda = 0.457\ \mu m$ and power $P = 80$ mW.

What might be surprising is that the giant-field fluctuations of the local fields and large SERS also occur for $\omega \ll \omega_p^*$, when the contrast, $H = |\varepsilon_m|/\varepsilon_d$, is large, $H \gg 1$, and a single metal grain does not resonate. To understand the origin of the giant-field fluctuations at $H \gg 1$, it is instructive first to consider the case when the metal concentration is exactly equal to the percolation threshold, $p = p_c$. Below, we develop a scaling approach to finding the local enhanced fields; this approach generalizes the known scaling arguments of the percolation theory (see, for example, Refs. 2 and 3).

To calculate the field distributions over the system at small losses ($\kappa = \varepsilon_m''/|\varepsilon_m'| \ll 1$), we apply the renormalization procedure based on dividing a system into squares of size l and considering each square as a new renormalized element. The effective dielectric constant of a conducting square, $\varepsilon_m^*(l)$, decreases with increasing size, l, as $\varepsilon_m^*(l) = (l/a_0)^{-t/\nu_p}\varepsilon_m$, whereas the effective dielectric constant of a dielectric square, $\varepsilon_d^*(l)$, increases with increasing l, as $\varepsilon_d^*(l) = (l/a_0)^{s/\nu_p}\varepsilon_d$, where t, s, and ν_p are the critical exponents for the static conductivity, dielectric constant, and the percolation correlation length, respectively ($t \approx s \approx \nu_p = 4/3$, for $d = 2$; see, for example, Ref. 2). We set now the square size, l, to be equal to $l = l^* = a_0(|\varepsilon_m'|/\varepsilon_d)^{\nu_p/(t+s)}$. Then, in the renormalized system, where each square of the size l^* is considered as a single element, the ratio of the dielectric constants of these new elements is equal to $\varepsilon_m^*(l^*)/\varepsilon_d^*(l^*) \cong \varepsilon_m/|\varepsilon_m'| = -1 + i\kappa$. Thus we return to the resonance situation (this time, for the renormalized elements); accordingly, the local electric fields, $E^*(l^*)$, are significantly enhanced in comparison with the applied field, E_0, in the renormalized system. The local fields, $E^*(l^*)$, are approximated as[8,15] $E^* \cong E_0\kappa^{-1/2} \gg E_0$.

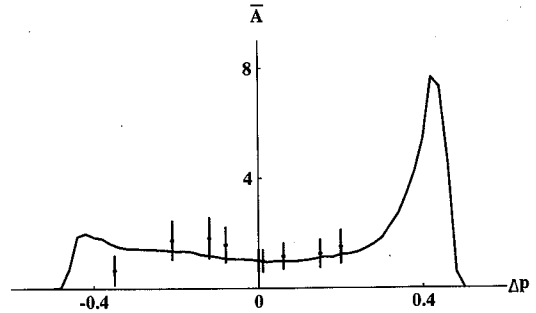

Fig. 2. Normalized SERS $\bar{A} = A/A_0$ as a function of the metal concentration, $\Delta p = p - p_c$, on a silver semicontinuous film. (The curve indicates theoretical calculations; the points indicate experimental data.)

Now we can estimate the field fluctuations in the original system. The field is still inhomogeneous for scales less than l^*. There are many finite-size metallic clusters, even inside of a square of the size l^*. For dielectric squares the voltage applied to a square drops mainly in the gaps between finite metal clusters, and therefore the largest fields are concentrated at the points where these clusters closely approach each other, so that the distances between the clusters are of the order of the grain size, a_0. Since the film is scale invariant at $p = p_c$, the number of such points, with closest approach of clusters, should not depend on the size l. A typical voltage drop, U^*, across a square of the size l^* is approximated as $U^* = E^*l^*$, and the local electric fields, $E_{\rm loc}$, concentrated at the points of closest approach can be estimated as $E_{\rm loc} \propto E^*l^*/a_0 \simeq E_0(|\varepsilon_m'|/\varepsilon_d)^{\nu_p/(t+s)}\kappa^{-1/2}$.

The presence of conducting squares does not change the above estimate since a conducting path does not affect much the largest fields in a square. Thus the averaged fourth power of the local fields is $\langle|E|^4\rangle \propto E_{\rm loc}{}^4/(l^*)^2 = E_0{}^4(|\varepsilon_m'|/\varepsilon_d)^{2\nu_p/(t+s)}\kappa^{-1}$. Since, as mentioned, the local fields are mainly concentrated in the dielectric gaps, we ultimately obtain from Eqs. (1) the following estimate for the Raman scattering enhancement at $p = p_c$:

$$A(p = p_c) = A_0 \propto (|\varepsilon_m'|/\varepsilon_d)^{2\nu_p/(t+s)}(|\varepsilon_m'|/\varepsilon_m''). \quad (2)$$

Substituting in Eq. (2) $t \approx s \approx \nu_p = 4/3$, we arrive at the following simple formula for the SERS in a two-dimensional percolating system:

$$A_0 \propto |\varepsilon_m'|^3/(\varepsilon_d\varepsilon_m''^2) \propto (\omega_p\tau)^2/\varepsilon_d, \quad (3)$$

where the latter relation is valid for the Drude metal at $\omega_p^* \gg \omega \gg \omega_\tau$. Our numerical calculations of $A_0(\omega)$ performed with the exact formula (1) are in excellent agreement with the $A_0(\omega)$ found from the scaling formula (3), for a wide spectral range, $\omega_p^* \gg \omega \gg \omega_\tau$ (results are not shown). The calculated average enhancement $A_0 \approx 10^6$, in the spectral range between 0.5 and 50μm. [To fit the numerical simulations we used in scaling formula (3) a prefactor, $c = 9.5$, that cannot, of course, be found from the simple scaling arguments used above.]

According to scaling formula (3), SERS at the percolation threshold is frequency independent in the spectral

range $\omega_p^* \gg \omega \gg \omega_\tau$. The distances ($\sim l^*$) between peaks in the Raman currents are $\propto \omega^{-1}$, whereas the peak amplitudes ($\propto E_{\rm loc}{}^4$) $\propto \omega^{-2}$, so that $A \propto E_{\rm loc}{}^4/(l^*)^2 \propto \omega^0$, in accordance with scaling formula (3). This behavior for the SERS peaks can be tracked in Fig. 1.

Equation (2) and formula (3) give the SERS enhancements at $p = p_c$. Indeed, they are also valid in some interval $\Delta p = p - p_c$ in a vicinity of p_c, when the size l^* is smaller than the percolation correlation length, $\xi_p \cong a_0|\Delta p|^{-\nu_p}$. Equating the values of l^* and ξ_p, we obtain the estimation for the concentration range where the SERS occurs: $\Delta p \leq \Delta^* = (\varepsilon_d/|\varepsilon_m'|)^{1/(t+s)}$. Based on this estimate, we propose the following scaling ansatz for the enhancement of Raman scattering:

$$A(p, \omega) = A_0(\omega)F(\Delta p/\Delta^*). \tag{4}$$

To find the scaling function $F(x)$, we calculated A for various ω and p. In our calculations we applied the described above RSRG method that was used for calculations of the local Raman signals (Fig. 1); the results were averaged over all the points (x, y) for ten random samples.

For very different frequencies used in our simulations the results collapse onto one curve $F(x)$ shown in Fig. 3. This function has first small maximum below p_c; at $p = p_c$ the function is $F(0) \approx 1$; then $F(x)$ has another larger maximum at $p > p_c$, and it finally vanishes, at $|\Delta p| > \Delta^*$. This double-peak behavior for $F(x)$ is associated with the discussed above evolution of the plasmon resonances with changing p and reflects the dependence of SERS on p shown in Fig. 2. The asymmetry in $F(x)$ is related to a simple fact that, while the local field distributions at some small p' and $1 - p'$ are qualitatively similar (resonances of metal grains and dielectric voids, respectively), the enhancement, A, in Eq. (1) is proportional to $|\varepsilon(x, y)|^2$ whose amplitude, on average, is larger at p close to 1 (recall that $|\varepsilon_m| \gg \varepsilon_d$).

In conclusion, we developed a scaling theory and performed numerical simulations for the local SERS distribution on a random metal-dielectric film. The distribution of local Stokes fields consists of well-separated peaks localized in nanometer-sized areas, with the positions depending on the laser frequency. The local SERS magnitudes in the peaks increase with wavelength as ω^{-2}, whereas the peaks separation is $\propto \omega^{-1}$. The local SERS in the peaks is much larger than the average SERS. The average enhancement of Raman scattering, A, is given, in a wide spectral range, by the simple formula $A = 9.5(\omega_p\tau)^2/\varepsilon_d \gg 1$, i.e., it is frequency independent. As a function of the metal concentration, the average enhancement A has a double-peak structure with the minimum at p_c.

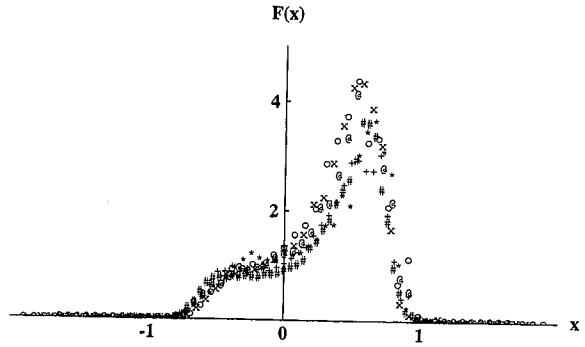

Fig. 3. SERS scaling function, $F(x)$, as a function of $x = (p - p_c)/\Delta^*$ [see Eq. (4)], for different wavelengths: $\lambda = 0.9\ \mu$m (#), $\lambda = 1.1\ \mu$m (+), $\lambda = 1.3\ \mu$m (*), $\lambda = 1.5\ \mu$m (@), $\lambda = 1.7\ \mu$m (x), and $\lambda = 1.9\ \mu$m (○).

REFERENCES

1. R. W. Cohen, G. D. Cody, M. D. Coutts, and B. Abeles, Phys. Rev. B **8**, 3689 (1973); G. A. Niklasson and C. G. Granqvist, J. Appl. Phys. **55**, 3382 (1984); Y. Yagil, P. Gadenne, C. Julien, and G. Deutscher, Phys. Rev. B **46**, 2503 (1992); P. Gadenne, A. Beghadi, and J. Lafait, Opt. Commun. **65**, 17 (1988).
2. D. J. Bergman and D. Stroud, Solid State Phys. **46**, 147 (1992); D. Stauffer and A. Aharony, *Introduction to Percolation Theory* (Taylor & Francis, Philadelphia, 1991).
3. F. Brouers, D. Rauw, J. P. Clerc, and G. Giraud, Phys. Rev. B **49**, 14582 (1994); J. P. Clerc, G. Giraud, and J. M. Luck, Adv. Phys. **39**, 191 (1990).
4. A. K. Sarychev, D. J. Bergman, and Y. Yagil, Phys. Rev. B **51**, 5366 (1995).
5. S. Nie and S. R. Emory, Science **275**, 1102 (1997).
6. K. Kneipp, Y. Wang, H. Kneip, L. Perelman, I. Itzkan, R. R. Dasari, and M. S. Feld, Phys. Rev. Lett. **78**, 1667 (1997).
7. M. Moskovits, Rev. Mod. Phys. **57**, 783 (1985); A. Otto, I. Mrozek, H. Grabhorn, and W. Akemann, J. Phys. C **4**, 1143 (1992); R. K. Chang and T. E. Furtak, eds., *Surface Enhanced Raman Scattering* (Plenum, New York, 1982); M. I. Stockman, V. M. Shalaev, M. Moskovits, R. Botet, and T. F. George, Phys. Rev. B **46**, 2821 (1992).
8. V. M. Shalaev, Phys. Rep. **272**, 61 (1996).
9. V. M. Shalaev, R. Botet, J. Mercer, and E. B. Stechel, Phys. Rev. B **54**, 8235 (1996); E. Y. Poliakov, V. M. Shalaev, V. A. Markel, and R. Botet, Opt. Lett. **21**, 1628 (1996).
10. V. A. Markel, L. S. Muratov, M. I. Stockman, and T. F. George, Phys. Rev. B **43**, 8183 (1991); M. I. Stockman, L. N. Pandey, L. S. Muratov, and T. F. George, Phys. Rev. Lett. **72**, 2486 (1994).
11. D. P. Tsai, J. Kovacs, Z. Wang, M. Moskovits, V. M. Shalaev, J. Suh, and R. Botet, Phys. Rev. Lett. **72**, 4149 (1994); V. M. Shalaev and M. Moskovits, Phys. Rev. Lett. **75**, 2451 (1995); S. I. Bozhevolnyi, I. I. Smolyaninov, and A. V. Zayats, Phys. Rev. B **51**, 17916 (1995).
12. E. Betzig and J. K. Trautman, Science **257**, 189 (1992); T. L. Ferrel, S. L. Sharp, and R. J. Warmack, Ultramicroscopy **42–44**, 408 (1992).
13. W. P. Ambrose, P. M. Goodwin, J. C. Martin, and R. A. Keller, Science **265**, 364 (1994); W. E. Moerner, T. Plakhotnik, T. Irngartinger, U. P. Wild, D. W. Pohl, and B. Hecht, Phys. Rev. Lett. **73**, 2764 (1994); C. Girard and A. Dereux, Rep. Prog. Phys. **59**, 657 (1996).
14. A. M. Dykhne, Sov. Phys. JETP **32**, 348 (1971).
15. F. Brouers, S. Blacher, and A. K. Sarychev, in *Fractals in the Natural and Applied Sciences* (Chapman & Hall, London, 1995), Chap. 24; F. Brouers, S. Blacher, A. N. Lagarkov, A. K. Sarychev, P. Gadenne, and V. M. Shalaev, Phys. Rev. B **55**, 13234 (1997).
16. P. J. Reynolds, W. Klein, and H. E. Stanley, J. Phys. C **10**, L167 (1977); A. K. Sarychev, Zk. Eksp. Teor. Fiz. **72**, 1001 (1977) [Sov. Phys. JETP **45**, 524 (1977)].
17. P. Gadenne, Y. Yagil, and G. Deutscher, J. Appl. Phys. **66**, 3019 (1989).
18. V. L. Schlegel and T. M. Corton, Ann. Chem. **63**, 241 (1991).